

Supporting information for

Conformational properties of biocompatible poly(2-ethyl-2-oxazoline)s in phosphate buffered saline

Alexander S. Gubarev^a, Bryn D. Monnery^b, Alexey A. Lezov^a, Ondrej Sedlacek^{b,c}, Nikolai V. Tsvetkov^a, Richard Hoogenboom^{b,*}, Sergey K. Filippov^{c,*}

S1. Experimental section

S1.1. Materials

Poly(2-ethyl-2-oxazoline)s were synthesized by living cationic ring-opening polymerization using optimized conditions to suppress chain transfer side reactions as previously reported.¹ ¹H-NMR was consistent with known values. Molar mass was determined by SEC-MALS. (Table S1)

Table S1. Molar masses of polymers analysis. a. Calculated from feed. b. Calculated by SEC-MALS

Ser No.	Nominal MW ^a	M _n ^b (kDa)	M _m ^b (kDa)	M _p ^b (kDa)	Đ ^b
P1	10 kDa	10.5	11.0	10.7	1.05
P2	20 kDa	18	18.8	18.7	1.04
P3	40 kDa	41.4	43.4	43.0	1.05
P4	60 kDa	56.2	62.5	66.0	1.11
P5	100 kDa	95.2	107.6	108.7	1.13
P6	200 kDa	183.2	216.5	215.9	1.18
P7	300 kDa	287.4	330.5	366.1	1.15

The molecular hydrodynamic methods (intrinsic viscosity, analytical ultracentrifugation, DLS, isothermal diffusion) were carried out in PBS buffer, which was prepared with ultrapure water obtained with Millipore (Direct-Q[®] 8 UV) and standard phosphate buffered saline tablets (1 tablet/200 ml), purchased from Sigma-Aldrich. The initial water was characterized with resistivity value of 18.5 MΩ cm and $pH = (6.77 \pm 0.04)$, which was determined at 25.0 °C with laboratory ionomer/conductometer/oxygenometer Anion-4151. The prepared PBS solution

showed $pH = (7.60 \pm 0.04)$ and no further pH value adjustments had been done. The densities and dynamic viscosities were experimentally determined and their values constituted as follows depending on the temperature: $\rho_0(25^\circ C) = 1.00398 \text{ g/cm}^3$, $\rho_0(37^\circ C) = 1.00012 \text{ g/cm}^3$ and $\eta_0(15^\circ C) = 1.153 \text{ cP}$, $\eta_0(25^\circ C) = 0.909 \text{ cP}$, $\eta_0(37^\circ C) = 0.709 \text{ cP}$, $\eta_0(45^\circ C) = 0.617 \text{ cP}$, $\eta_0(55^\circ C) = 0.528 \text{ cP}$, consequently.

S2. Methods.

S2.1 Size Exclusion Chromatography

Size-exclusion chromatography (SEC) was performed on an Agilent 1260-series HPLC system equipped with a 1260 online degasser, a 1260 ISO-pump, a 1260 automatic liquid sampler (ALS), a thermostatted column compartment (TCC) at $50^\circ C$ equipped with two PLgel $5 \mu\text{m}$ mixed-D columns and a precolumn in series, a 1260 diode array detector (DAD) and a 1260 refractive index detector (RID). The used eluent was DMA containing 50mM of LiCl at a flow rate of 0.500 ml/min. A multi-angle light scattering detector (Wyatt Dawn Heleos II) was added to the system. Samples were filtered ($0.2 \mu\text{m}$ PTFE filter) prior to injection. A differential refractometer (Wyatt Optilab T-rEX) was used to determine the d_n/d_c value of the polymer. Wyatt ASTRA 7 was used to process the data.

S2.2. Viscometry measurements

Intrinsic viscosities $[\eta]$ were determined with the data obtained using of a Lovis 2000 M microviscometer (Anton Paar GmbH, Graz, Austria). The experiments were based on the rolling ball (Höppler) principle; standard dilution procedures were used. The setup included a capillary with an inner diameter of 1.59 mm equipped with a gold-coated steel ball (1.50 mm in diameter). The rolling times for a solvent (t_0) and polymer solutions of various concentrations (t) were measured at a tilting angle of the capillary of 50° within the wide temperature range (15, 25, 37, 45 and $55^\circ C$). The values of relative viscosity $\eta_r = \eta/\eta_0 = t/t_0$ were determined. The concentration dependences of specific viscosity η_{sp} normalized by concentration c ($\eta_{sp}/c = (t/t_0 - 1)/c$) as well as $\ln \eta_r/c$ were extrapolated to zero concentration. The dependences for extremely diluted polymer solutions in the $1.2 < t/t_0 < 2.5$ range were approximated by straight lines (Fig. S1 SI); the intercept values correspond to intrinsic viscosity $[\eta]$ of a solution, according to the Huggins and Kraemer equations.³⁻⁴ Finally the values $[\eta]$ obtained in such manner were averaged and used for further analysis (Table 1 and Table S2).

S2.2 Analytical ultracentrifugation

Sedimentation velocity experiments were performed with a ProteomeLab XLI Protein Characterization System analytical ultracentrifuge (Beckman Coulter, Brea, CA), using conventional double-sector Epon or aluminum centerpieces of 12 mm optical path length and a four-hole rotor (An-60Ti). Rotor speed was 40 000 – 55 000 rpm, depending on the sample.

Cells were filled with 420 μL of a sample solution and 440 μL of the PBS buffer. Before the run, the rotor was thermostated for approximately 1 h at 37 $^{\circ}\text{C}$ in the centrifuge. Sedimentation profiles were obtained at the same temperature, using interference optics.

For the analysis of the sedimentation velocity data, $c(s)$ model with a Tikhonov–Phillips regularization procedure implemented into the Sedfit program was applied.⁵

The $c(s)$ analysis is based on the numerical solution of the Lamm equation assuming the averaging frictional ratio (f/f_{sph}) values for all sedimenting species. An example of the data evaluation by Sedfit is shown in Fig. S2.

At least three concentrations of each sample were studied, covering a wide concentration range ($3 \leq c_{max}/c_{min} \leq 7$). The parameter $c[\eta]$ characterizing the degree of dilution was in the range of $0.008 \leq c[\eta] \leq 0.1$, corresponding to a high dilution state; this, in turn, allows for reliable extrapolation to the zero concentration. Respectively, the evaluated velocity sedimentation coefficients and the frictional ratios were extrapolated using corresponding linear approximations:

$$s^{-1} = s_0^{-1}(1 + k_s c) \quad 1$$

$$f/f_{sph} = (f/f_{sph})_0(1 + k_f c) \quad 2$$

where s_0 and $(f/f_{sph})_0$ are extrapolated values of the sedimentation coefficients and the frictional ratios correspondingly, k_s is the concentration sedimentation parameter (Gralen coefficient) and k_f is the concentration frictional ratio parameter. The corresponding concentration dependences of the sedimentation coefficients and the frictional ratios are presented in Fig. S2.

S2.3 Dynamic Light Scattering

Dynamic light scattering experiments were performed using a “Photocor Complex” instrument (Photocor Instruments Inc., Moscow, Russia) equipped with a real-time correlator (288 channels, the fastest sample-time 10 ns) in the 30 – 140 $^{\circ}$ scattering angle ϑ range within the wide temperature range (15, 37, 55 and up to 65 $^{\circ}\text{C}$); temperature stabilization is ± 0.1 $^{\circ}\text{C}$; the wavelengths of laser light sources (λ_0) are 405 and 654 nm. The cell (cylindrical glass cell 1 cm in diameter) with a studied solution or solvent was submerged in an immersion liquid (decane) having the same refractive index as the cell glass. The normalized intensity homodyne autocorrelation functions were fitted using the ILT regularization procedure incorporated in ‘DynaLS’ software (which provides distributions of relaxation times and hydrodynamic radii).⁶⁻⁷ Since all the observed modes displayed diffusional nature ($1/\tau = D \times q^2$), the values of the translational diffusion coefficients D were calculated from the slope of linear dependence of inverse relaxation time $1/\tau$ on scattering vector squared $q^2 = (4\pi n \lambda_0^{-1} \sin(\vartheta/2))^2$. The

translational diffusion coefficients D_0 corresponding to infinite dilution limit were determined by extrapolation to zero concentration (Fig. S3).

S2.4 Isothermal Diffusion Measurements

The translational diffusion was as well studied by the classical method of a solvent/solution boundary formation.⁸ The diffusion boundary was created in a glass cell with a thickness of $h = 30 \text{ mm}$ along the beam path, at average solution concentration of $c = 0.6 \text{ mg ml}^{-1}$. Lebedev's polarizing interferometer with a digital matrix was used as an optical system for the observation of the position of the solvent/solution boundary.⁹ The experiments were performed at $T = 37 \text{ }^\circ\text{C}$. The translational diffusion coefficients were calculated by the following equation:

$$\sigma^2 = \sigma_0^2 + 2Dt \quad 3$$

where σ^2 is the dispersion of the diffusion boundary calculated from the maximum ordinate and the area under the diffusion curve, σ_0^2 is the zero dispersion characterizing the quality of the boundary formation, and t is the diffusion time. In **Fig. S3** the corresponding dependences of the diffusion dispersion σ^2 over the time t are shown. The evaluated values of the diffusion coefficients D were assumed to be the values extrapolated to the zero concentration; the data are summarized in **Table 1** and **Table S3** (*vide infra*).

Alternatively, the diffusion coefficients might be determined based on the sedimentation velocity data. The $c(s)$ analysis implemented into Sedfit is based on the numerical solution of the Lamm equation.⁵ By this approach, the translation diffusion coefficient is initially expressed in terms of the frictional ratio $(f/f_{sph})_0$, where f is a translational frictional coefficient of the studied macromolecule and f_{sph} is the one of an equivalent sphere. The translational diffusion coefficient D can then be calculated as:

$$D_0 = \frac{k_B T (1 - v\rho_0)^{1/2}}{\eta_0^{3/2} 9\pi\sqrt{2} ((f/f_{sph})_0)^{3/2} (s_0 v)^{1/2}} \quad 4$$

where η_0 – dynamic viscosity of the solvent, ρ_0 – density of the solvent, k_B – Boltzmann constant, T – the absolute temperature, v – partial specific volume

Heretofore, was demonstrated, that for various polymer systems the diffusion coefficients evaluated by this approach are indeed truthful and adequate, making the sedimentation velocity analysis completely independent and self-sufficient tool for the molar mass/size determination.¹⁰⁻¹³ At the same time for a number of more complex macromolecular systems with more pronounced non-ideality behavior as well as rigid chain polymers this approach may fall short in its accuracy and suitability.¹¹

The in here found values of D based on the frictional ratios were found to be well correlated with the ones determined by the isothermal diffusion and DLS experiments. Hence, in further calculations of the associated properties of the PEtOx macromolecules the average values of the

diffusion coefficients determined by the three independent techniques were used. It is worth noticing, that such a comparison of the equivalent hydrodynamic characteristic made by different approaches represents a fundamental task of establishing the inter-correlation of the used methods as well as making the value determination more accurate. The overall summary of the individual values of the diffusion coefficients and the frictional ratios can be seen in **Table S3**.

S2.5 Partial Specific Volume and Refractive Index Increment

The density measurements were carried out in pure water at $T = 37\text{ }^\circ\text{C}$, using the density meter DMA 5000 M (Anton Paar GmbH, Graz, Austria) and according to the procedure of Kratky *et al.*¹⁴ The corresponding dependence of $\Delta\rho = \rho - \rho_0$ on the polymer concentration c is shown in **(Figure S4a)**. The value of the partial specific volume was calculated as $\Delta\rho/\Delta c = (1 - v\rho_0)$ and constitutes $v = 0.853 \pm 0.001\text{ cm}^3\text{g}^{-1}$.

The refractive index increment **(Figure S5b)** can be calculated knowing the number of the interference fringes (J), determined from the sedimentation velocity experiments:

$$\frac{dn}{dc} = \left(\frac{J}{c}\right)\frac{\lambda}{l} \quad 5$$

where c – is the concentration, λ – wavelength (655 nm) and l is the optical path length (12 mm). The calculated value of $dn/dc = 0.15 \pm 0.01\text{ cm}^3\text{g}^{-1}$ is in good correlation with the value evaluated by the isothermal diffusion measurements $0.14 \pm 0.01\text{ cm}^3\text{g}^{-1}$.

S3. Experimental data (The sedimentation-diffusion analysis of the absolute values of the molar masses)

Based on the results of performed hydrodynamic experiments with linear PEtOx series, the self-consistency check of hydrodynamic characteristic must be checked. To do so, the characteristics should be expressed as intrinsic values which are independent from the common solvent properties – dynamic viscosity and density:

$$[\eta] = \Phi_0 \frac{\langle h^2 \rangle^{3/2}}{M} \quad 6$$

$$[s] \equiv \frac{s_0 \eta_0}{(1 - v\rho_0)} = \frac{M}{N_A P_0 \langle h^2 \rangle^{1/2}} \quad 7$$

$$[D] \equiv \frac{D_0 \eta_0}{T} = \frac{k_B}{P_0 \langle h^2 \rangle^{1/2}} \quad 8$$

$$k_s = B \frac{\langle h^2 \rangle^{3/2}}{M}, \quad 9$$

where $\Phi_0 = 2.86 \times 10^{23}$ and $P_0 = 5.11$ are Flory parameters, $B = B(L/A, d/A)$ is a dimensionless parameter depending on hydrodynamic interactions in the sedimenting solute, L – contour length of a polymer chain, A – equilibrium rigidity and M – molar mass.

Each of these characteristics is related with the same basic macromolecular parameters, such as molar mass and end to end distance of a polymer chain $\langle h^2 \rangle$ or hydrodynamic size. The analysis of the mutual intercorrelation of the hydrodynamic parameters can be established by calculation of the hydrodynamic invariant A_0 and the sedimentation parameter β_s :¹⁵⁻¹⁶

$$A_0 = (R[s][D]^2[\eta])^{\frac{1}{3}} \quad 10$$

$$\beta_s = k_B^{-\frac{2}{3}} (N_A[s][D]^2 k_s)^{\frac{1}{3}} \quad 11$$

where R – universal gas constant, N_A – Avogadro's number.

Low fluctuations of the A_0 and β_s values around their averages allow to state that the satisfactory correlations between the molecular characteristics $([\eta], [s], [D], k_s)$ revealed from the independent measurements are achieved, which, in turn, enables further interpretation of the experimental data. The average values of A_0 and β_s were found to be $3.03 \pm 0.05 \times 10^{-10} \text{ g cm s}^{-2} \text{ K}^{-1} \text{ mol}^{-1/3}$ and $1.20 \pm 0.02 \times 10^7 \text{ mol}^{-1/3}$, respectively. The determined values fall within physically sounded range which is known for the flexible linear chain polymers in good solvent.^{15, 17} Thus, the absolute values of the molar mass can be calculated based on the determined values of the sedimentation coefficient and the diffusion coefficients using the Svedberg equation:

$$M_{sD} = \frac{s_0 RT}{D_0(1 - v\rho_0)} = \frac{[s]}{[D]} R \quad 12$$

For linear polymer molecules the dimensions of the corresponding polymer coil in solution can, exemplarily, be represented by the hydrodynamic size. However, such estimations will be based on the radius of a hydrodynamic equivalent sphere and can differ much from the size of the actual macromolecule in the solution. The more precise representation of the molecular size will be given by the end to end distance of the polymer chain $\langle h^2 \rangle^{1/2}$ and can be calculated *via*:

$$\langle h^2 \rangle_{[s][\eta]}^{1/2} = \left(N_A [s] [\eta] \frac{P_0}{\Phi_0} \right)^{1/2} \quad 13$$

or if the translation diffusion data is used *via*:

$$\langle h^2 \rangle_{[D]}^{1/2} = \frac{k_B}{P[D]}$$

The calculated average values of $\langle h^2 \rangle^{1/2}$ are also shown in the **Table 1**.

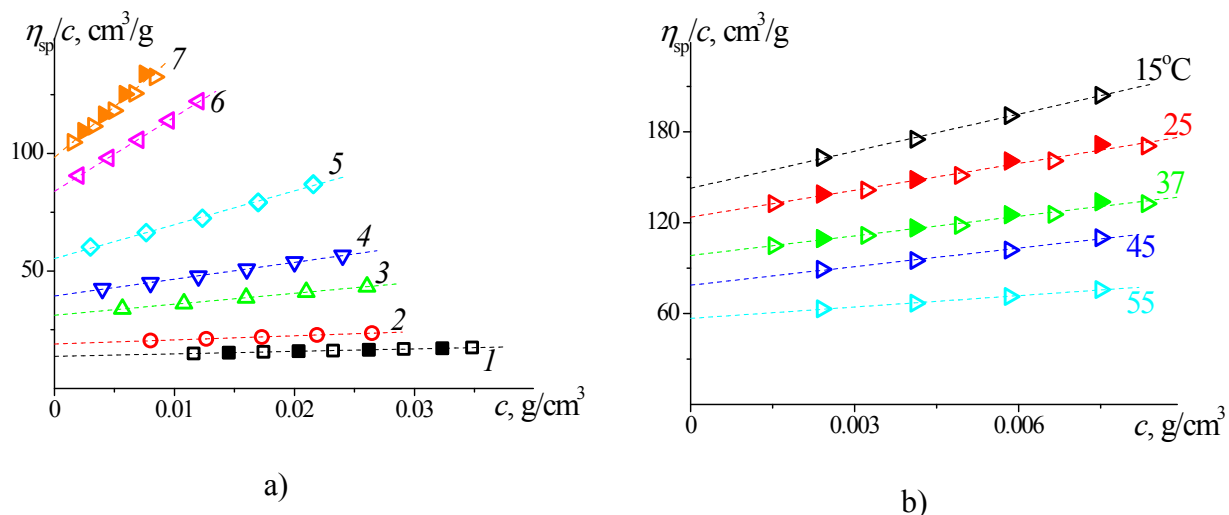
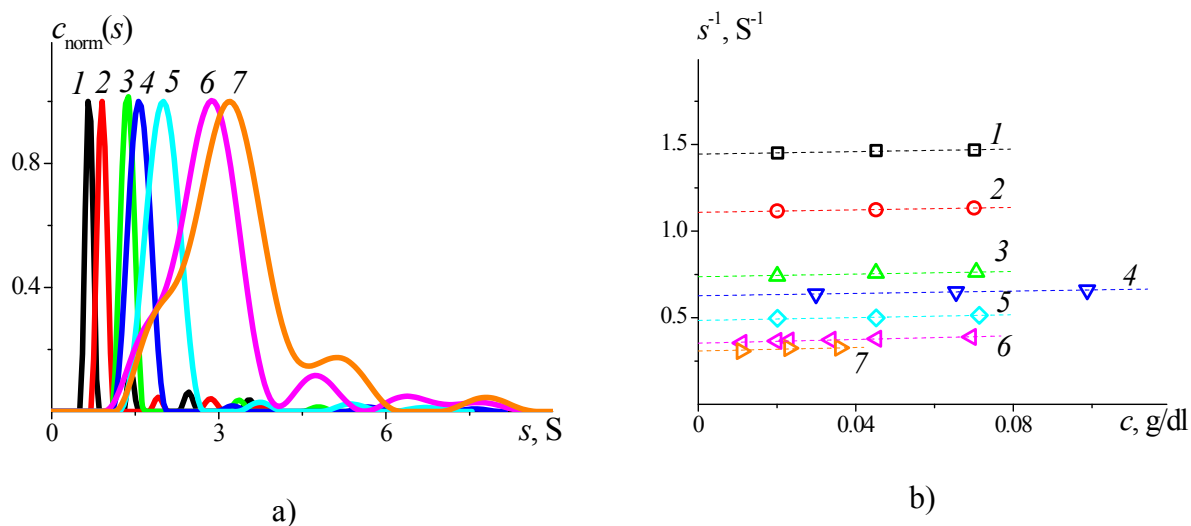
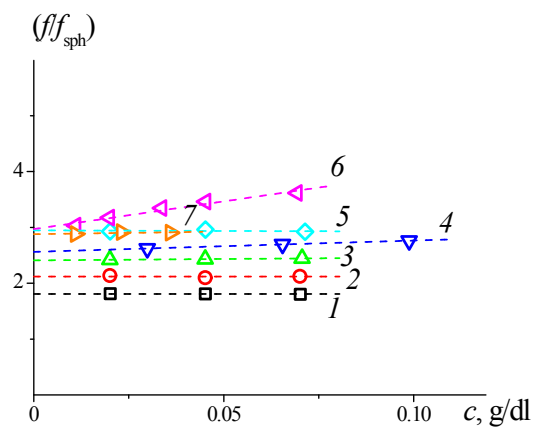


Figure S1. The dependence of η_{sp}/c on c for all studied samples (a) and for sample 7 at all studied temperatures (b). The open and filled symbols correspond to the same systems, but the measured solutions were prepared independently. The numbering next to the lines at (a) correspond to sample numbers in Table 1 and at (b) – the temperatures are shown.





c)

Figure S2. The obtained sedimentation coefficients distributions (a) and concentration dependence of acquired sedimentation coefficients as well as frictional ratios (c) for all studied samples at 37 °C.

Table S2. The intrinsic viscosity values $[\eta]$, Huggins k' and Kraemer k'' coefficients of PETOx samples in PBS solutions determined within wide temperature range.

Sample	15 °C		25 °C		37 °C		45 °C		55 °C	
	$[\eta]$, cm ³ /g	$k'/$ $-k''$								
P1	16.7	0.47/ 0.09	15.4	0.51/ 0.07	13.8	0.57/ 0.04	12.6	0.62/ 0.01	11.4	0.68/ -0.04
P2	-	-	21.5	0.44/ 0.11	19.0	0.49/ 0.08	-	-	-	-
P3	40.9	0.40/ 0.13	36.6	0.43/ 0.12	31.4	0.48/ 0.10	27.8	0.54/ 0.07	23.3	0.65/ 0.01
P4	-	-	46.7	0.41/ 0.12	39.6	0.46/ 0.11	-	-	-	-
P5	75.6	0.38/ 0.13	67.2	0.40/ 0.13	55.7	0.47/ 0.11	47.6	0.55/ 0.07	37.2	0.73/ 0.001
P6	-	-	104.6	0.39/ 0.13	84.4	0.45/ 0.11	-	-	-	-
P7	143	0.40/ 0.13	124	0.38/ 0.13	99	0.45/ 0.11	79.8	0.66/ 0.02	57.4	0.77/ -0.08

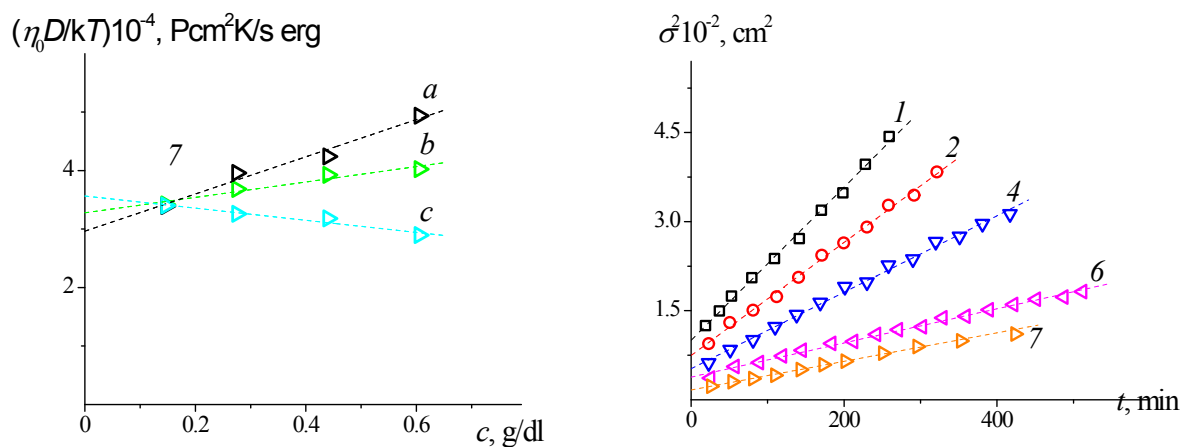


Figure S3. Diffusion coefficients determined in DLS (a) and isothermal diffusion coefficient measurements (b). The numbers next to the dependences correspond to the sample numbers.

Table S3. Diffusion coefficients and frictional ratios values of PEtOx samples in PBS solutions at 37°C determined with different techniques.

	$D_0^1 10^7$, cm	$D_0^2 10^7$, cm	$(f/f_{sph})_0^3$	$D_{sf}^3 10^7$, cm	$\langle D_0 \rangle 10^7$, cm
P1	10.7	10.0	1.81	11.6	10.8
P2	8.1	8.4	2.12	8.0	8.2
P3	-	5.7	2.41	5.4	5.6
P4	5.0	4.6	2.56	4.6	4.7
P5	-	3.5	2.94	3.3	3.4
P6	2.4	2.4	2.97	2.7	2.5
P7	2.0	2.0	2.9	2.6	2.2

¹ – the data of isothermal translational diffusion experiments; ² – DLS; ³ – sedimentation velocity experiments data.

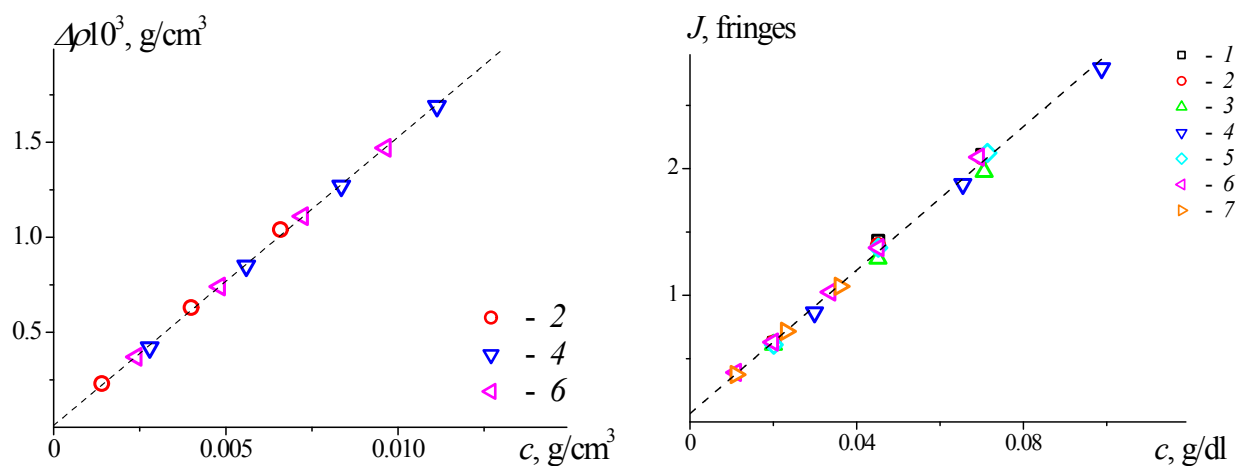


Figure S4. The dependences of $\Delta\rho$ and interference fringes (J) on concentrations c of PEtOx samples in PBS solutions at 37 °C. The numbers at the graphs correspond to the sample numbers.

Table S4. The parameters of the KMHS relationships for PEtOx samples in PBS solutions different temperatures.

$P_i - P_j$	$T, ^\circ\text{C}$	$b_{ij} \pm \Delta b_{ij}$	K_{ij}	r
$[\eta] - M$	15	0.68 ± 0.01	0.029	0.99991
	25	0.67 ± 0.01	0.030	0.99990
	37	0.63 ± 0.01	0.038	0.99992
	45	0.59 ± 0.01	0.052	0.99996
	55	0.51 ± 0.01	0.093	0.99972
$s_0 - M$	37	0.49 ± 0.01	0.007	0.99984
$D_0 - M$		-0.51 ± 0.01	1260	-0.99968
$s_0 - [\eta]$		0.78 ± 0.01	0.090	0.99969
$D_0 - [\eta]$		-0.81 ± 0.01	89.6	-0.99964
$s_0 - D_0$		-0.97 ± 0.01	7.0	-0.99915
$k_s - s_0$		1.24 ± 0.08	36.3	0.99049

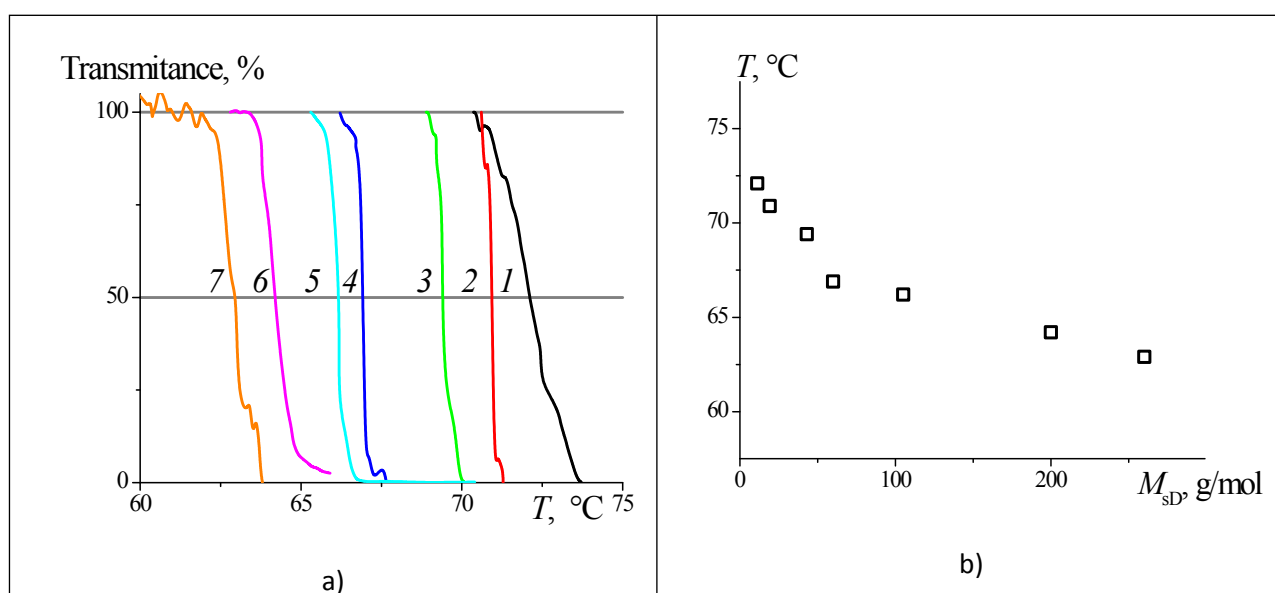


Figure S5. Temperature dependence of the transmittance for PetOx samples in PBS solutions. The numbers next to the dependences correspond to sample numbers (a). Dependence of cloud point against molecular mass M_{SD} for PetOx samples in PBS solution (b).

The phase behavior of PEtOx solutions above 60° C was investigated by DLS technique. The sample was equilibrated at 60 °C, and then heated with the rate 0.1° per minute with the measurement of the DLS autocorrelation functions at $\theta = 90^\circ$, a peak with a maximum in the region of 1 μm appeared.

Temperature dependence of normalized intensity distribution function on hydrodynamic radii R_h is presented on figure S6. The height of the peaks in the distribution is presented by color gradations, in accordance with the insert in the right side of the Figure S6. In accordance with the experimental data the peak with a maximum close to the 1 μm appears at temperatures higher than 62.5 °C and its fraction rapidly growth with the increasing of the solution temperature. The appearance of the large particles in the solution indicates a beginning of the phase separation process, which accompanied by aggregation of individual PEtOx macromolecules into large aggregates.

It should also be noted that the DLS method is more sensitive to a large particles in solution ($I \sim M \sim V \sim R^3$), and therefore Figure S6 characterizes only the initial period of water PEtOx solution separation when the fraction of aggregates in solution is small.

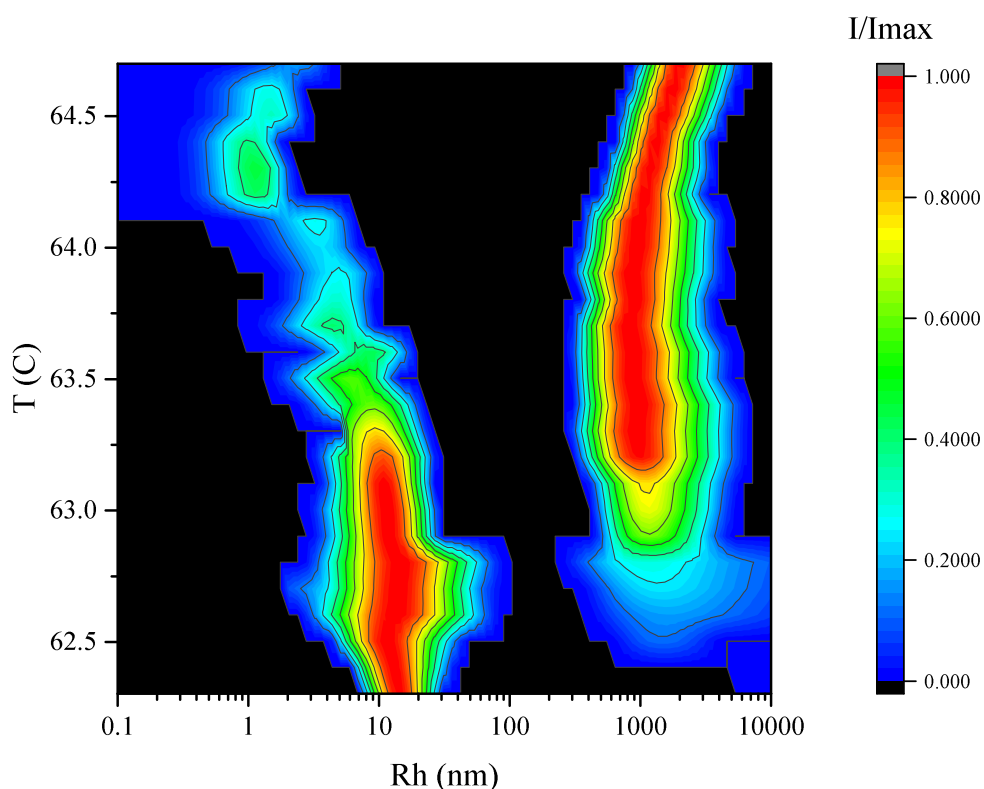


Figure S6. Temperature dependence of normalized scattered light intensity distributions.

References:

1. Monnery, B. D.; Hoogenboom, R. Method for the preparation of uniform high molar mass cyclic imino ether polymers. PCT / EP2015 / 065 829, 2015.
2. Hoogenboom, R.; Monnery, B., Method for the preparation of uniform, high molar mass cyclic imino ether polymers. Google Patents: 2016.
3. Huggins, M. L., The Viscosity of Dilute Solutions of Long-Chain Molecules. IV. Dependence on Concentration. *J. Am. Chem. Soc.* **1942**, *64* (11), 2716-2718.
4. Kraemer, E. O., Molecular Weights of Celluloses and Cellulose Derivates. *Ind. Eng. Chem.* **1938**, *30* (10), 1200-1203.
5. Schuck, P., Size-distribution analysis of macromolecules by sedimentation velocity ultracentrifugation and lamm equation modeling. *Biophys. J.* **2000**, *78*, 1606-19.
6. Berne, B. J.; Pecora, R., *Dynamic Light Scattering: With Applications to Chemistry, Biology, and Physics*. Dover Publications: 2013.
7. <http://www.photocor.ru/dynals>.
8. Tsvetkov, V. N.; Eskin, V. E.; Frenkel, S. Y., *Structure of macromolecules in solution*. Nat. Lend. Library Sci.&Technol.: Boston, 1971.
9. Lavrenko, V. P.; Gubarev, A. S.; Lavrenko, P. N.; Okatova, O. V.; Pavlov, G. M.; Panarin, E. F., Processing of Digital Interference Images Obtained on Tsvetkov Diffusometer. *Indus. Lab.* **2013**, *79* (7-1), 33-36.
10. Pavlov, G. M.; Perevyazko, I.; Schubert, U. S., Velocity Sedimentation and Intrinsic Viscosity Analysis of Polystyrene Standards with a Wide Range of Molar Masses. *Macromol. Chem. Phys.* **2010**, *211*, 1298-1310.
11. Pavlov, G. M.; Perevyazko, I. Y.; Okatova, O. V.; Schubert, U. S., Conformation parameters of linear macromolecules from velocity sedimentation and other hydrodynamic methods. *Methods* **2011**, *54*, 124-135.
12. Pavlov, G. M., Different Levels of Self-Sufficiency of the Velocity Sedimentation Method in the Study of Linear Macromolecules. In *Analytical Ultracentrifugation: Instrumentation, Software, and Applications*, Uchiyama, S.; Arisaka, F.; Stafford, F. W.; Laue, T., Eds. Springer Japan: Tokyo, 2016; pp 269-307.
13. Nischang, I.; Perevyazko, I.; Majdanski, T.; Vitz, J.; Festag, G.; Schubert, U. S., Hydrodynamic Analysis Resolves the Pharmaceutically-Relevant Absolute Molar Mass and Solution Properties of Synthetic Poly(ethylene glycol)s Created by Varying Initiation Sites. *Anal. Chem.* **2017**, *89* (2), 1185-1193.
14. Kratky, O.; Leopold, H.; Stabinger, H., The determination of the partial specific volume of proteins by the mechanical oscillator technique. *Methods Enzymol.* **1973**, *27*, 98-110.
15. Tsvetkov, V. N.; Lavrenko, P. N.; Bushin, S. V., Hydrodynamic Invariant of Polymer-Molecules. *J. Polym. Sci., Part A: Polym. Chem.* **1984**, *22* (11), 3447-3486.
16. Pavlov, G.; Frenkel, S., Sedimentation parameter of linear polymers. *Prog. Colloid Polym. Sci.* **1995**, *99*, 101-108.
17. Pavlov, G. M.; Frenkel, S. Y., The sedimentation parameter of linear polymer molecules in absence of excluded volume effects. *Acta Polym.* **1988**, *39*, 107-111.